ELSEVIER

Coordination Chemistry Reviews
159 (1997) 245–255

COORDINATION CHEMISTRY REVIEWS

Light-induced multielectron charge transfer processes occurring in a series of Group-8–platinum cyanobridged complexes

Ying Wu, Brian W. Pfennig, Stefanie L. Sharp, David R. Ludwig, Christopher J. Warren, Edward P. Vicenzi, Andrew B. Bocarsly *

Chemistry Department, Princeton University, Princeton, NJ 08544-1009, USA

Received 22 December 1995

Contents

Abstract

Although true multielectron charge transfer processes do not exist within the realm of molecular photochemistry, one can design mimicking systems via the production of a reactive one-electron charge transfer intermediate. Reported in this review are the photochemical and photophysical properties of a group of symmetric, multinuclear complexes of the general form $[L'(CN)_4M(CN)$–(PtL_4)–(NC)–$M(CN)_4L']^{n-}$ (where M is a Group 8 metal, L is an amine, and L′ is a σ-donor ligand) that provide for apparent photoinduced multielectron charge transfer. These complexes exhibit intense intervalence charge transfer (IVCT) bands

* Corresponding author.

PII S0010-8545(96)01290-8

in the blue portion of the optical spectrum (350–450 nm). In the case where M = Fe, irradiation into the IVCT band centered at 425 nm produces a net two-electron charge transfer with a quantum yield of ca. 0.1 in an aqueous solvent. However, multielectron charge transfer photochemistry can be observed for M = Os or Ru only by using a mixed DMSO–aqueous solvent, in which the cyanide to water hydrogen bonding found in pure aqueous solvent is destroyed, thereby, shifting the redox potential of the cyanometalates to values similar to M = Fe. The observed reaction is found to selectively yield two-electron products. The reactivity of these complexes as a function of Group 8 metal and solvent system is nicely predicted using the charge transfer theories of Marcus and Hush, with the source of the differential reactivity being the shift in the relative activation barriers for the conversion of a one-electron [Fe^{III}, Pt^{III}, Fe^{II}] intermediate to the observed two-electron products or to the starting material. Well-defined oligomers and polymers of the iron-based system have been synthesized. The photochemical reactivity and photophysics of these species are found to be a function of molecular geometry. In the case of the polymeric systems, one-dimensional, two-dimensional, and network materials can be synthesized using electrochemical techniques to control the polymer reactivity sites. Both solution and surface-confined photochemistry can be observed for these systems. © 1997 Elsevier Science S.A.

Keywords: Group-8–cyanobridged complex; Photochemical reactivity; Photophysics; IVCT bands

1. Introduction

The practical application of converting optical energy to chemical energy via a redox-type mechanism lies in the ability of the chemical system to transfer more than one electron upon light absorption. In the effort to develop molecular systems that are capable of transferring more than one electron, two different pathways have been explored. One approach is to assemble a large number of chromophores into a supramolecular system [1–5] through suitable chelating or spacer ligands, or by polymeric backbones [6]. In such systems, multiple electron transfer is achieved by sequential absorption of multiple photons by linked chromophores. However, with each absorption event, only one electron is transferred at the most. A second approach is to utilize charge transfer reactions that differ by more than one electron, so that multiple electrons can be transferred upon absorption of one photon [7], a so-called photoinduced multielectron charge transfer process.

In view of this second approach, platinum seems to be ideally suited because it forms stable oxidation states in its complexes of Pt(II) and Pt(IV), while Pt(III) species are typically unstable and short-lived. The complex of interest must be able to photochemically convert the Pt oxidation state from one of the stable states to the other. In such a conversion process, the unstable Pt(III) state is inevitably generated, assuming a stepwise electron transfer mechanism. Once this occurs, a rapid follow up thermal reaction back to one of the stable oxidation states is expected to occur. This thermal reaction will either regenerate the initial oxidation state, leading to no net chemistry, or produce an oxidation state that varies by two electrons from the reactant. It is this latter process that is of interest to provide a

pathway to customized systems that are capable of two-electron charge transfer upon one-photon absorption.

2. Preparation of molecular species capable of multielectron charge transfer

Following the above strategies, we reported the syntheses of a group of trinuclear complexes of the form $\{L(CN)_4M^{II}\text{–}(CN)\text{–}Pt(L')_4\text{–}(NC)\text{–}M^{II}(CN)_4L\}^{n-}$, where M = Fe, Ru, or Os, $L = CN^-$ or a σ-donor ligand, and $L' = NH_3$ or ethylenediamine (en) [8–11]. A structural diagram of the complex where, M = Fe, $L = CN^-$, and L'_2 = en is shown in Fig. 1. These compounds were found to exhibit an intense absorption in the visible spectral region. The absorption band was found to disappear upon oxidation of M(II) to M(III), and the energy of the absorption maximum varied with the change in the redox potential of the 'M(CN)$_5$L' moiety brought about by the variations in M and L. Based on these observations, this low energy absorption band was assigned as an intervalence charge transfer (IVCT) band.

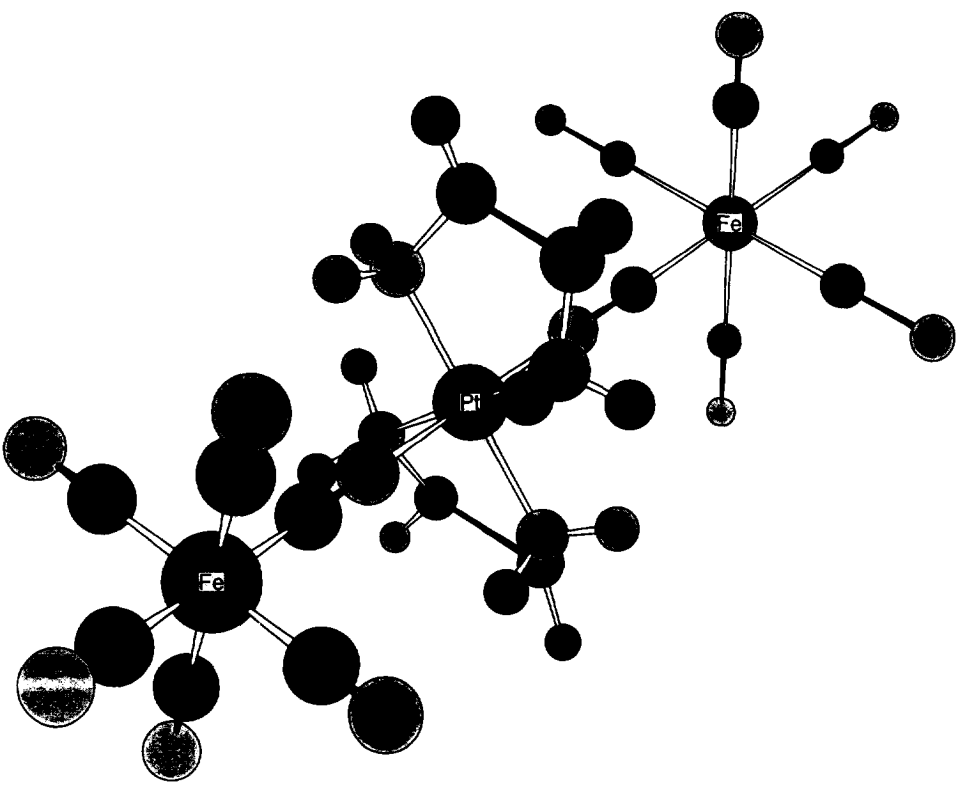

Fig. 1. Computer model of the trimetallic species, $\{(CN)_5Fe^{II}\text{–}(CN)\text{–}Pt^{IV}(en)_2\text{–}(NC)\text{–}Fe^{II}(CN)_5\}^{4-}$ (en = ethylenediamine). This model is based on spectroscopic data and a crystal structure of the analogous complex in which amino ligands are substituted for en.

2.1. Theoretical basis of the IVCT: Marcus–Hush theory

The theory of optically induced electron transfer developed by Marcus and coworkers [12–14] and Hush [15–17] has been widely and successfully applied to many dinuclear species [18–20]. Although the electron transfer process in our system involves two electrons and three metal centers, the observed sensitivity of the photoinduced charge transfer to the metal center's redox potentials suggests that the chemistry can still be described using the Marcus–Hush theory which states that

$$E_{op} = \Delta E + \lambda_{vib} + \lambda_{solvent} \quad (1)$$

where E_{op} is the energy of the optically induced electron transfer process, ΔE is the energy difference between the ground states of the metal centers, and λ_{vib} and $\lambda_{solvent}$ are the molecular vibrational reorganization and solvent reorganization energies. In the case of the trinuclear complexes discussed here, the three redox sites are represented by three overlapping parabolas, as shown in Fig. 2. The quantum yield for the two-electron process depends on the crossing points of the three parabolas, which are determined by the relative zero points of the three potential wells. These crossing points set the activation barriers of the non-productive back reaction from the Pt(III) state E_{a1} and the productive forward reaction E_{a2} that results in net two-electron transfer. In the case where M = Fe, irradiation into the IVCT band produces a net two-electron charge transfer with a quantum yield of ca. 0.1 (at 488 nm), when the complex is dissolved in an aqueous solvent. However, if Os or Ru are substituted for the Fe centers, no photochemistry is observed upon irradiation into the IVCT band, even over prolonged irradiation times.

Note that the high energy nature of the one-electron transfer state precludes the formation of one-electron products as a possible side reaction.

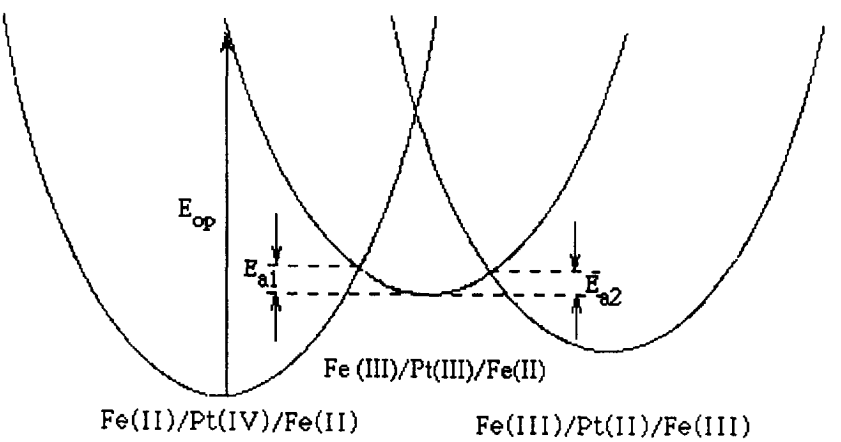

Fig. 2. Illustration of potential energy wells for $[(NC)_5Fe–(CN)–PtL_4–NC–Fe(CN)_5]^{4-}$ and related species.

2.2. The application of charge transfer theory to the trinuclear system

The Marcus–Hush theory on electron transfer is manifested in the following of factors that control the energetics of the IVCT transition.

2.2.1. Inner sphere factors

The first term in Eq. (1) has to do with the relative redox potential of the metal centers involved in the charge transfer process. The difference in the particular cyanometalate moiety used, as well as the difference in ligands associated with the metal centers, are expected to change the redox potentials of the metal centers and thus alter the ΔE term, shifting the light-induced IVCT energy. In order to evaluate this effect, two series of complexes were studied, one being the $[(NC)_5M(CN)$–$Pt(NH_3)_4$–$(NC)M(CN)_5]$ series where M = Fe, Ru, or Os, and the other being the $\{L(CN)_4Fe(CN)$–$Pt(NH_3)_4$–$(NC)Fe(CN)_4L\}^{n-}$ series where L is a σ-donor ligand [10]. In both cases the optical energy required to induce the electron transfer was found to be linearly related to the difference in ground state redox energies of the M and Pt complexes, validating the use of Eq. (1). From these data, reasonable estimates of reorganization energies and thermal activation barriers have been calculated and reported. Overall, the reorganization energy was found to be on the order of ca. 160 kJ mol^{-1}.

2.2.2. Outer sphere factors

The second sphere coordination between the solvent molecules and the ligands can sometimes significantly change the redox property of certain metal complexes. In the case studied here, the magnitude of ΔE can be affected by the solvent employed due to the high level of hydrogen bonding which can occur between the cyanometalates and good hydrogen donor (lone pair acceptor) solvents. Solvents such as water, which are better electron pair acceptors than aprotic solvents such as DMSO, can accept electron density more efficiently from the lone pairs on the cyanide nitrogen atoms. This lowers the energy of the cyanide π^* molecular orbitals, facilitating the M–C backbonding. In turn, the cyanometalate complex becomes more difficult to oxidize under these conditions. In contrast, the redox potential of the coordinatively saturated Pt moiety should not be significantly shifted by changing the solvent, since no electron lone pairs are available to interact with the second coordination sphere. By mixing solvents such as H_2O and DMSO, a continuum of solvent hydrogen bonding ability was generated, and the redox potential of the Fe center was modified. At a certain point, the free energy for the oxidation of the Fe(II) by Pt(IV) shifts to positive values, and the charge transfer process is shut off. Thus, both the thermal and photochemical redox reactivity of these systems are solvent gated. The ability of DMSO to shift redox potential of the cyanometalate moiety is most pronounced in the case where M = Os. In pure aqueous solvent, no productive photochemistry was observed upon irradiation of the solution. However, with the addition of DMSO, the redox potential shifted negative to the region observed for the M = Fe system, and productive photochemistry was apparent [10].

The solvent-gated photochemistry was employed in the process of deriving a

mathematical relationship between the quantum yield Φ and the redox potentials [11]. By using different DMSO/H_2O ratios, the term ΔE in Eq. (1) was shifted systematically, and the quantum yield at different ΔE values were measured. By applying the Marcus–Hush model, the following relationship between Φ and redox potentials was derived.

$$\frac{1}{\Phi} = A \exp\left[-\ln\frac{k}{\nu_n} - \frac{[E_{op}^2/(E_{op} - \Delta E_1)]}{RT} \right] + B \tag{2}$$

where A and B are constants determined by the Arrhenius constants, k is the rate constant for the formation of the trinuclear complex, ΔE_1 is the difference between the bottom of the energy wells Fe^{II}–Pt^{IV}–$Fe^{II} \rightarrow Fe^{III}$–$Pt^{III}$–$Fe^{II}$ and Fe^{III}–Pt^{III}–$Fe^{II} \rightarrow Fe^{III}$–$Pt^{II}$–$Fe^{III}$ (Fig. 2) respectively, which can be calculated from the redox potentials of the redox centers involved. This equation makes it possible to predict the quantum yield of the two-electron process by knowing the positions of the bottom points of the potential energy wells.

It is also of interest to study the effect of neat organic solvents on the energetics of the charge transfer process; however, the complexes studied in the above two series were soluble only in aqueous solvent. To remedy this problem, the complex $\{(NC)_5Fe(CN)Pt(en)_2(NC)Fe(CN)_5\}^{4-}$ was synthesized [11]. This complex not only dissolves in aqueous solutions, like the parent complex, but also in a variety of neat organic solvents, thereby allowing for an unambiguous analysis of the solvent dependence on the photophysics and photochemistry of the IVCT transition. The IVCT energy of the complex in different solvents was correlated to the electron-accepting ability and the dielectric constants of the solvents used via Gutman's acceptor number scale [11]. It was found that in order for the complex to dissolve, a large dielectric constant is required of the solvent to support the substantial charge on the complex. Once dissolved, a linear relationship was found between the IVCT energy and the acceptor number of the solvent, as shown in Fig. 3. A higher acceptor number is associated with an improved ability to hydrogen bond to the cyanide lone pair electrons. This hydrogen bonding interaction is very important in determining the ground state redox potential of the $[Fe(CN)_6]^{3-/4-}$ moiety, and thus the optical transition energy. The observed solvatochromic behavior can thus be understood as a consequence of the shift in the free energy of the charge transfer reaction.

2.2.3. Temperature dependence of the IVCT transition [11]

The temperature dependence of IVCT transition was also investigated for M = Fe. The redox potential of the Fe center was found to vary as temperature changes, which inevitably leads to a temperature-dependent IVCT band energy. Assuming all the terms in Eq. (1) may be viewed as free energies, the temperature dependence of the charge transfer process can be equated to the entropy of the reaction. It was calculated that the entropy change for the one-electron reduction of Pt was $\Delta S = -205 \pm 14\ J\ mol^{-1}\ K^{-1}$. The large negative value of the entropy change associated with the redox event at the Pt center indicates that the formation of the Pt(III) species is entropically unfavored.

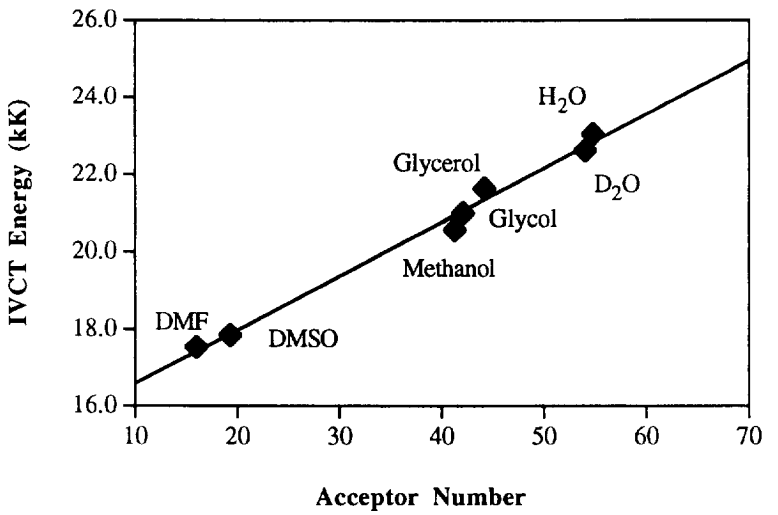

Fig. 3. Correlation between the IVCT band energy and the electron-accepting ability of the solvents.

3. Formation of redox polymers based on the trinuclear species

3.1. Electrochemical polymerization

Having established a chromophoric unit capable of one-photon–two-electron processes, the possibility of generating redox polymers based on these units was undertaken. The synthetic approach involved electrochemically oxidizing the Fe(II) centers giving rise to $[Fe^{III}–Pt^{IV}–Fe^{III}]^{2-}$ species, which could then oxidize free $[Pt(NH_3)_4]^{2+}$ to form polymers consisting of repeating $[Fe^{II}(CN)_6–Pt^{IV}(NH_3)_4]$ units (Eqs. (3) and (4)).

$$n[Fe^{II}–Pt^{IV}–Fe^{II}] \xrightarrow{[ox]} n[Fe^{III}–Pt^{IV}–Fe^{III}] \xrightarrow{nPt^{II}} [Fe^{II}–Pt^{IV}]_{2n} \quad (3)$$

$$2[Fe^{II}–Pt^{IV}]_n \xrightarrow{[ox]} 2[Fe^{III}–Pt^{IV}]_n \xrightarrow{Pt^{II}} [Fe^{II}–Pt^{IV}]_{2n+1} \quad (4)$$

It was found that this polymerization strategy could be carried out at a variety of electrode surfaces, including nickel, platinum, and optically transparent indium–tin oxide (ITO) to produce polymer films which adhered to the electrode [21]. The common feature observed in all three cases was that the cyclic voltammogram of the film derivatized at 1.4 V vs. a saturated calomel electrode (SCE) shows four sets of waves (Fig. 4) although the $[Fe–Pt–Fe]^{4-}$ in solution yields only one set of two-electron peaks at 0.54 V vs. SCE. The increased number of peaks found in the cyclic voltammogram of the polymer-modified surface was indicative of an increased ratio of bridging cyanide to Fe centers. The $Fe^{II/III}$ redox potential is strongly dependent on the number of bridging –CN– ligands associated with a particular Fe center. Based on these facts, the waves at 0.54, 0.82, 1.05, and 1.27 V vs. SCE are assigned

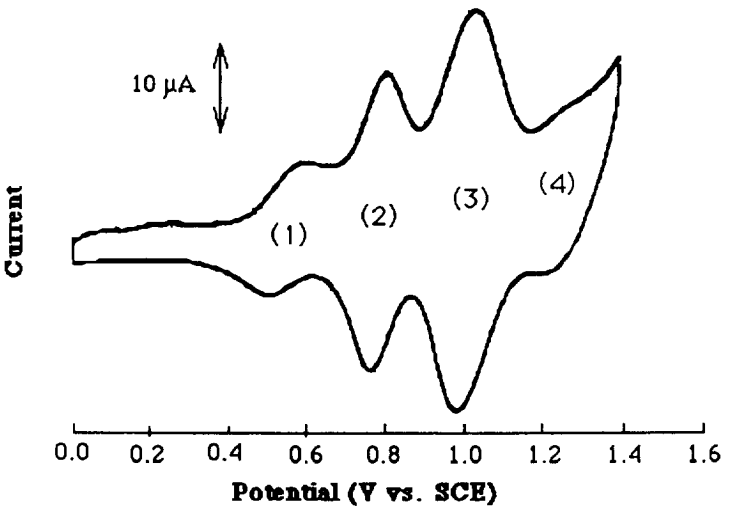

Fig. 4. Cyclic voltammogram of an ITO electrode derivatized at 1.4 V vs. SCE (scan rate, 50 mV s^{-1}; electrolyte, 0.5 M $NaNO_3$). The sets of redox waves numbered (1)–(4) corresponds to the redox events of Fe centers with 1, 2, 3, and 4 bridging cyanide ligands respectively.

to the redox events of Fe centers with 1, 2, 3, and 4 bridging cyanide ligands respectively. The dependence of the $Fe^{II/III}$ redox potential on the number of bridging cyanides offered a means to control the degree of crosslinking in the polymer through the control of derivatizing potential, since a higher crosslinked system requires a more positive potential to keep the polymerization process going. The more extensive bridging allows for the generation of two- or even three-dimensional structures, leading to a polymeric film of reasonable thickness.

3.2. Photochemical pattern formation on redox polymer derivatized electrode interfaces

Photolysis experiments performed on dry films revealed that films derivatized at 1.4 V vs. SCE were photochemically inactive. In this case, the high degree of crosslinking is likely to allow for a high degree of bond reformation. A less oxidizing potential of 1.0 V vs. SCE was found to be suitable to generate a polymeric film of good stability and reasonable thickness while preserving the photodissociation properties of the monomeric unit [21]. Based on the known photodissociation of the trinuclear Fe–Pt–Fe complex, the light-induced polymer dissociation is assumed to take place via the following pathway:

$$[Fe^{II}\text{–}Pt^{IV}]_{2n+1} \xrightarrow{h\nu} 2[Fe^{III}\text{–}Pt^{IV}]_n + [Pt(NH_3)_4]^{2+} \quad (5)$$

or

$$[Fe^{II}\text{–}Pt^{IV}]_n \xrightarrow{h\nu} n[Fe(CN)_6]^{3-} + n[Pt(NH_3)_4]^{2+} \quad (6)$$

In order for the photolysis to be productive, the polymer films needed to be irradiated in an aqueous solution. The irradiated film undergoes cleavage of the N–Pt bond (Eqs. (5) and (6)). When a Ni electrode was used, the photoproduct, $[Pt(NH_3)_4]^{2+}$, dissolved in the solution, leaving behind nickel ferricyanide as a precipitate at the electrode interface. In the case of ITO, both photoproducts, $[Pt(NH_3)_4]^{2+}$ and $[Fe(CN)_6]^{3-}$, dissolve in the surrounding solution, leading to the complete dissolution of the film in the irradiated area. However, at the ITO electrode interface, the photogenerated ferricyanide may be precipitated if a second transition metal cation is present in the vicinity of the electrode surface. Thus, mixed-metal cyanometalate species could be generated photochemically by adding a second transition metal cation to the solution in which the electrode is immersed during photolysis. The presence of such species on the electrode surface was evidenced by microscopic FTIR data [21].

Owing to the photoinduced nature of the formation of mixed-metal cyanometalates, masking techniques were employed to selectively irradiate certain areas on the electrode surface, generating micrometer-scale lateral structures. In addition, since the different cyanometalates have their own unique absorption properties, the structural variation on the electrode surface was also visible to the eye, appearing as patterns that are duplicates of the mask [21].

The ability to generate multicomponent electrode surfaces is particularly of interest to us in view of new developments in fabricating microstructures on chemically modified electrode surfaces [22–27]. Several experimental techniques involving multiple electrochemical–photochemical steps have recently been reported [28–30]. Our procedure described above provides an addition to the already developed techniques in that it only requires one photochemical step to directly generate the second desired component on the electrode surface; no follow up chemistry is necessary.

4. Application of a patterned electrode interface as a light modulating device: development of a 'molecular Venetian blind'

By utilizing the photochemical pattern formation discussed above, and incorporating the electrochromic properties of certain cyanometalates, we were able to produce a 'molecular Venetian blind', a striped electrode surface that is able to reversibly change color. A striped mask was used to generate a stripe pattern at the electrode interface, with alternating regions of $[Fe–Pt]_n$ polymer and mixed-metal cyanometalate. In one specific case when the polymer derivatized electrode was irradiated in a solution of 0.1 M $Fe(NH_4)_2(SO_4)_2$, Fe^{2+} was incorporated into the ferricyanide lattice, forming Prussian blue (PB), giving rise to an electrode surface with alternating blue and light yellow stripes.

Detailed analysis of the surface composition of a derivatized ITO electrode with photogenerated mixed-metal cyanometalate was carried out using the electron probe microanalysis (EPMA) technique [31,32]. The EMPA method employs a primary beam of focused electrons that cause target atoms to reach an excited state via inner

shell electron ionization. During relaxation process, X-rays characteristic of the target atoms are emitted, allowing for both qualitative and quantitative analysis. The quantitative analysis of Pt and the incorporated metal cation across the stripes reveals periodic changes in the concentrations. Line-scan profiles show a rather constant concentration of Fe composition across the electrode, but a significant decrease in Pt concentration, mirrored by an increase in M^{n+} concentration in the photolyzed areas, was observed [21], generating a periodic concentration profile which mimics the photolysis mask.

The patterned surface can act as a diffraction grating for red light, since red light is absorbed by the photogenerated PB due to its IVCT centered at 710 nm, while the $[Fe–Pt]_n$ film is transparent in this spectral region. When a beam from a He–Ne laser (633 nm) is passed through such an electrode, diffraction out to the fifth-order bands was clearly visible [21]. The stripe spacing calculated based on the diffraction pattern is in good agreement with the band width on the mask and the width measured from the electron probe micrograph. As the optical absorption of the PB film can be easily altered by changing the electrode potential, this diffraction grating can be turned 'on' and 'off' through the control of potential. When the applied bias is such that all Fe centers in PB are in either the +2 oxidation state or the +3 oxidation state, it no longer has an intervalence electron transfer transition, and thus does not absorb in the red. As a result, outside the PB potential window (0.25–0.90 V vs. SCE), the entire electrode surface becomes transparent to red light and the diffraction pattern disappears. Visually, the blue stripes on the electrode surface fade away. Good electrochemical reversibility was established by repeated cycling of potential. The derivatized layer is air stable and requires no special care.

With the feasibility of such a 'molecular Venetian blind' demonstrated, one can easily envision the possibility of custom designing dynamic diffraction gratings specific to certain wavelengths through the choice of cyanometalates that fit desired absorption requirements.

Acknowledgements

The work presented here was supported by the United States National Science Foundation under Grant No. CHE-9312056.

References

[1] V. Balzani, F. Scandola, M.A. Fox and M. Chanon (Eds.), Photoinduced Electron Transfer, Elsevier, Amsterdam, 1988.
[2] V. Balzani, F. Barigelletti and L. De Cola, Topics Curr. Chem., 158 (1990) 31.
[3] V. Balzani, Pure Appl. Chem., 62 (1990) 1099.
[4] V. Balzani and F. Scandola, Supramolecular Photochemistry, Ellis Horwood, West Sussex, 1991.
[5] F. Scandola, M.T. Indelli, C. Chiorboli and C.A. Bignozzi, Topics Curr. Chem., 158 (1990) 73.
[6] L.A. Worl, G.F. Strouse, J.N. Younathan, S.M. Baxter and T.J. Meyer, J. Am. Chem. Soc., 112 (1990) 7571.

[7] A. Sykes, Kinetics of Inorganic Reactions, Pergamon, Oxford, 1966.
[8] M. Zhou, B.W. Pfennig, J. Steiger, D. Van Engen and A.B. Bocarsly, Inorg. Chem., 29 (1990) 2457.
[9] B.W. Pfennig and A.B. Bocarsly, Coord. Chem. Rev., 111 (1991) 91.
[10] B.W. Pfennig and A.B. Bocarsly, J. Phys. Chem., 96 (1992) 226.
[11] Y. Wu, C. Cohran and A.B. Bocarsly, Inorg. Chim. Acta, 226 (1994) 251.
[12] R.A. Marcus, J. Chem. Phys., 24 (1956) 966.
[13] R.A. Marcus, J. Chem. Phys., 43, (1965) 679.
[14] R.A. Marcus and N. Sutin, Inorg. Chem., 14 (1975) 213.
[15] N.S. Hush, Trans. Faraday Soc., 57 (1956) 557.
[16] N.S. Hush, Prog. Inorg. Chem., 8 (1957) 357.
[17] N.S. Hush, Chem. Phys., 10 (1975) 361.
[18] T.J. Meyer, Acc. Chem. Res., 11 (1978) 94.
[19] A. Vogler, A.H. Osman and H. Kunkely, Coord. Chem. Rev., 64 (1985) 159.
[20] C. Creutz, Prog. Inorg. Chem., 30 (1989) 1.
[21] Y. Wu, B.W. Pfennig, E.P. Vicenzi and A.B. Bocarsly, Inorg. Chem., 34 (1995) 4262.
[22] M.S. Wrighton, Science, 231 (1986) 32.
[23] C.E. Chidsey and R.W. Murray, Science, 231 (1986) 25.
[24] R.W. Murray, A.G. Ewing and R.A. Durst, Anal. Chem., 59 (1987) 379A.
[25] R.W. Murray (Ed.), Molecular Design of Electrode Surfaces, Wiley, New York, 1992.
[26] M.J. Natan and M.S. Wrighton, Prog. Inorg. Chem., 37 (1989) 391.
[27] M.D. Ryan, E.F. Bowden and J.Q. Chambers, Anal. Chem., 66 (1994) 360R.
[28] S. Gould, K.H. Gray, R.W. Linton and T.J. Meyer, Inorg. Chem., 31 (1992) 5521.
[29] M.-N. Callomb-Dunand-Sauthier, A. Doronzier and R. Ziessel, J. Phys. Chem., 97 (1993) 5973.
[30] S. Gould, T.R. O'Toole and T.J. Meyer, J. Am. Chem. Soc., 12 (1990) 9490.
[31] J.L. Pouchou and F. Pichoir, Rech. Aerosp., 5 (1984) 349.
[32] J.L. Pouchou and F.M.A. Pichoir, Microbeam Anal., 23 (1988) 315.